Asymmetric double barrier resonant tunnelling structures with improved characteristics

Jun-jie Shi*[1,3], Barry C. Sanders[1] and Shao-hua Pan[1,2,3]
[1] Department of Physics, Macquarie University, Sydney, New South Wales 2109, Australia
[2] Institute of Physics, Chinese Academy of Sciences, P. O. Box 603, Beijing 100080, P. R. China
[3] China Center of Advanced Science and Technology (World Laboratory), P. O. Box 8730, Beijing 100080, P. R. China

(February 7, 2008)

We present a self-consistent calculation, based on the global coherent tunnelling model, and show that structural asymmetry of double barrier resonant tunnelling structures significantly modifies the current-voltage characteristics compared to the symmetric structures. In particular, a suitably designed asymmetric structure can produce much larger peak current and absolute value of the negative differential conductivity than its commonly used symmetric counterpart.

73.40.Gk, 73.23.Hk

Significant progress in the growth of semiconductor materials has re-invigorated research in double-barrier resonant tunnelling structures (DBRTSs) and their applications [1]. The key feature of the DBRTS [2] which promises benefits is the negative differential resistance (NDR) [3]. For example, the NDR can be exploited in high-speed analog-to-digital converters [4] and parity generators [5]. We propose asymmetric structure design to improve the DBRTS characteristics, in particular the peak current and the NDR. We show that an appropriate asymmetric design can yield improved characteristics. Our simulation employs the self-consistent global coherent tunnelling model which is valid at and near the resonance bias.

In the global coherent tunnelling model we can express the three-dimensional electronic wave function for a DBRTS as a product of the bulk Bloch wave function and a one-dimensional envelope wave function $\psi_{E_z}(z)$ along the growth axis (z) of the DBRTS, satisfying the Schrödinger equation

$$-\frac{\hbar^2}{2}\frac{d}{dz}\left[\frac{1}{m(z)}\frac{d}{dz}\psi_{E_z}(z)\right]+\left[V(z)-e\Phi(z)\right]\psi_{E_z}(z) = E_z\psi_{E_z}(z), \tag{1}$$

with $m(z)$ the electron effective mass, $-e$ the electron charge, $V(z)$ the conduction-band offset, and $\Phi(z)$ the Hartree potential satisfying the Poisson equation

$$\frac{d}{dz}\left[\epsilon(z)\frac{d\Phi(z)}{dz}\right] = -e\left[N_D^+(z)-n(z)\right], \tag{2}$$

where $\epsilon(z)$ is the dielectric constant, $N_D^+(z)$ is the density of ionised donors, and $n(z)$ is the electron density which can be expressed as

$$n(z) = n^{(E\to C)}(z)+n^{(C\to E)}(z). \tag{3}$$

Here $n^{(E\to C)}(z)$ ($n^{(C\to E)}(z)$) is the density of electrons tunnelling from the emitter to collector (from the collector to emitter). In the following we write explicitly only for $n^{(E\to C)}(z)$, and $n^{(C\to E)}(z)$ can be treated similarly.

$$n^{(E\to C)}(z) = \frac{L_E k_B T}{\pi^2\hbar^3}\left(\frac{m_E}{2}\right)^{3/2} \times\int_0^\infty \frac{\ln\{1+\exp[(E_F-E_z)/k_BT]\}}{\sqrt{E_z}} \times\left|\frac{1}{\sqrt{B}}\psi_{E_z}^{(E\to C)}(z)\right|^2 dE_z, \tag{4}$$

where L_E is the emitter length, k_B and T are, respectively, the Boltzmann constant and temperature, E_F is the Fermi energy level, and m_E is the electron effective mass in the emitter. In our iterative numerical calculation for self-consistent solutions of the coupled Schrödinger and Poisson equations, the normalization constant B is determined by

$$B = \frac{k_B T}{\pi^2\hbar^3 n^{(E)}}\left(\frac{m_E}{2}\right)^{3/2} \times\int_0^\infty \frac{\ln\{1+\exp[(E_F-E_z)/k_BT]\}}{\sqrt{E_z}}dE_z \times\int_0^L \left|\psi_{E_z}^{(E\to C)}(z)\right|^2 dz, \tag{5}$$

where $n^{(E)}$ is the dopant density in the emitter and L is the entire length of the DBRTS including the emitter and collector. Equation (5) is derived from the requirement of electric charge neutrality, namely $\int_0^L n^{(E\to C)}(z)dz = L_E n^{(E)}$. A similar treatment for self-consistent solutions has been used by Zimmermann et al. [6]. Our numerical calculations show that such a normalisation method ensures fast convergence of the solution. It is worth mentioning that the appearance of L_E and $n^{(E)}$ on Eqs. (4) and (5) implies that the density of tunneling electrons depends on the parameters of electron reservoir. In our numerical calculations, a standard iteration algorithm has been used: Eq. (1) is solved with a transfer matrix method [7], and Eq. (2) is solved in the subsequent iterations with Dirichlet boundary conditions, which keep the values of the potential at the two boundaries fixed.

We present our numerical results for the following DBRTSs: $\mathcal{S}(L_E, d_w, d_r; x)$=$n^+$GaAs($L_E$)/GaAs(4nm)-/$Al_xGa_{1-x}As$(3nm)/GaAs($d_w$)/$Al_{0.3}Ga_{0.7}As$($d_r$)/-GaAs(4nm)/$n^+$GaAs($L_E$). The emitter and collector are assumed to be of equal lengths, and the doping concentration is assumed to be $n^{(E,C)} = 10^{18}$ cm^{-3}. Calculations are all performed at $T = 300$ K. The electron effective mass in $Al_xGa_{1-x}As$ is $m = (0.0665 + 0.0835x)m_0$ with m_0 the free electron mass. The conduction-band discontinuity between the GaAs and $Al_xGa_{1-x}As$ is given by $V(x) = 0.6(1266x + 260x^2)$ meV. The relative dielectric constant in $Al_xGa_{1-x}As$ is $13.18 - 3.12x$.

Figure 1 presents current-voltage curves for DBRTSs $S(10\text{nm}, 5\text{nm}, d_r; 0.3)$ with the right-barrier thickness $d_r = 2$, 3 and 4 nm. The figure shows that the asymmetric structure with a narrower right barrier ($d_r = 2$ nm) has a higher peak current (I_p) than the symmetric one ($d_r = 3$ nm). The trend of increasing I_p with decreasing d_r, shown in the figure, is consistent with recent experimental results [8]. This is because the peak transmission coefficient of the electron is higher for a structure with narrower right barrier. Moreover, Fig. 1 shows that the peak position moves towards higher bias voltage for a DBRTS with thicker right barrier. This trend is also consistent with previous experimental results [8]. However, due to neglect of phase-coherence breaking scattering, the present simple model cannot explain the decreasing peak-to-valley ratio (PVR) with increasing right barrier width, which was observed by previous authors and was attributed to the increase of the valley current and change of PVR caused by electron-electron scattering [8].

Figure 2 presents calculated results for DBRTSs $S(10\text{nm}, 5\text{nm}, 3\text{nm}; x)$ with the left-barrier Al mole $x = 0.2$, 0.3 and 0.4. The figure shows that the peak current and absolute value of the negative differential conductivity are higher for a structure with lower x and hence lower left barrier. Although we have not found previously published experimental data to test the above calculated results, we can attribute the above trend to two physical reasons. First, a structure with a lower left barrier has a higher peak transmission coefficient. Secondly, the bias raises the left barrier top to the right one. A structure with a lower left barrier can compensate the latter effect and hence can cause the left and right barrier tops to locate at similar energy levels under resonant bias. For example, the left and right barrier tops in the $x = 0.2$ asymmetric DBRTS under resonance bias are closer than that in the symmetric one with $x = 0.3$. As is known, a DBRTS with the same or similar left and right barrier potential can achieve enhanced transmission coefficient. Based on the above two physical reasons, we can understand why the peak currents and absolute value of the negative differential conductivities of the structures with $x = 0.2$, 0.3 and 0.4 have such a large difference as shown in Fig. 2. In particular, the peak current and absolute value of the negative differential conductivity for the asymmetric structure with $x = 0.2$ are much larger than that of the symmetric one ($x = 0.3$). Such asymmetric structural effect, which is favorable to some device applications of DBRTSs, await experimental confirmation.

Incidentally, in our calculations shown in Figs. 1 and 2 we have set the emitter length $L_E = 10$ nm. This scale is somewhat shorter than that in commonly-used DBRTSs. However, some authors prefer a shorter emitter, e.g., $L_E = 5$ nm in Ref. [9] and in Fig. 2.7 of Ref. [10].

Besides the above study on the role of asymmetry between the left and right barriers, we have also investigated the size effect of the quantum well width d_w. The calculations show that the peak current increases and the peak position shifts to a higher bias voltage if the well width decreases, which is in agreement with the previous experiments [11]. As for the size effect of the emitter (collector) length L_E, our calculations show that when the emitter length L_E decreases, the electron accumulation in the quantum well becomes smaller which gives rise to a weaker self-consistent field resulting in a smaller band bending, and hence the peak current increases with decreasing the emitter (collector) length L_E. The reduction of peak current with increasing emitter length is obvious for $L_E \leq 10$ nm and is shown in Fig. 3, while it is less obvious for larger L_E (say $L_E > 20$ nm) and is not shown here.

In summary, our self-consistent calculations show that the resonant tunnelling current depends sensitively on and hence can be effectively controlled by structure parameters, such as the barrier heigths and widths of the left and right barriers, and the well width. An asymmetric DBRTS with a suitably designed structure has a much larger peak current and absolute value of the negative differential conductivity than the commonly used symmetric one. Moreover, the size effect of the emitter (collector) length is theoretically studied and explained for the first time.

[1] Sun, J.P., Haddad, G.I., Mazumder, P. and Schulman, J.N., *Proc. IEEE.* **86**, 1998, 641.

[2] Tsu, R. and Esaki, L., *Appl. Phys. Lett.* **22**, 1973, 562; Chang, L.L., Esaki, L. and Tsu, R., *Appl. Phys. Lett.* **24**, 1974, 593.

[3] Sollner, T.C.L.G., Goodhue, W.D., Tannenwald, P.E., Parker, C.D. and Peck, D.D., *Appl. Phys. Lett.* **43**, 1983, 588.

[4] Sen, S., Capasso, F., Cho, A.Y., and Sivco, D., *IEEE Tran. Electron Devices*, **34**, 1987, 2185.

[5] Capasso, F., Sen, S., Beltram, F., Lunardi, L.M., Vengurlekar, A.S., Smith, P.R., Shah, N.J., Malik, R.J., and Cho, A.Y., *IEEE Tran. Electron Devices*, **36**, 1989, 2065.

[6] Zimmermann, B., Marclay, E., llegems, M. and Gueret, P., *J. Appl. Phys.* **64**, 1988, 3581.

[7] Shi, J.-J., Sanders, B.C. and Pan, S.-H., *Euro. Phys. Journal B* **4**, 1998, 113.

[8] Schmidt, T., Tewordt, M., Haug, R.J., Klitzing, K.V., Schönherr, B., Grambow, P., Förster, A. and Lüth, H., *Appl. Phys. Lett.* **68**, 1996, 838.
[9] Lake, R. and Datta, S., *Phys. Rev. B* **45**, 1992, 6670.
[10] Mizuta, H. and Tanoue, T., *The Physics and Applications of Resonant Tunnelling Diodes*, Cambridge University Press, Cambridge, 1995, p. 23.
[11] Teitsworth, S.W., Turley, P.J., Wallis, C.R., Li, W. and Bhattacharya, P.K., *Semicond. Sci. Technol.* **9**, 1994, 508.

FIG. 1. Current-voltage curves for DBRTSs n^+GaAs(10nm)/GaAs(4nm)/$Al_{0.3}Ga_{0.7}As$(3nm)/ GaAs(5nm)/$Al_{0.3}Ga_{0.7}As(d_r)$/GaAs(4nm)/n^+GaAs(10nm). The solid, dash and dash-dot lines are for d_r = 2, 3 and 4 nm, respectively.

FIG. 2. Current-voltage curves for DBRTSs n^+GaAs(10nm)/GaAs(4nm)/$Al_xGa_{1-x}As$(3nm)/ GaAs(5nm)/$Al_{0.3}Ga_{0.7}As$(3nm)/GaAs(4nm)/n^+GaAs(10nm). The solid, dash and dash-dot lines are for x = 0.2, 0.3 and 0.4, respectively.

FIG. 3. Current-voltage curves for DBRTSs n^+GaAs(L_E)/GaAs(4nm)/$Al_{0.3}Ga_{0.7}As$(3nm)/ GaAs(5nm)/$Al_{0.3}Ga_{0.7}As$(3nm)/GaAs(4nm)/n^+GaAs(L_E). The solid, dash and dash-dot lines are for L_E = 5, 8 and 10 nm, respectively.

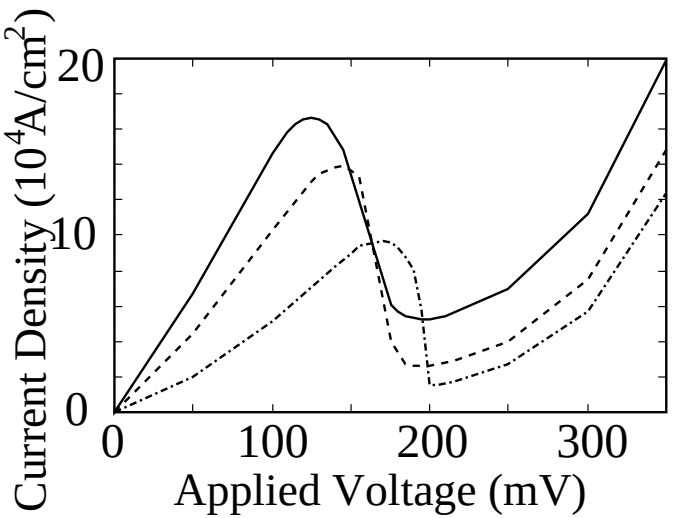

Fig. 1
Shi et al.
SSC

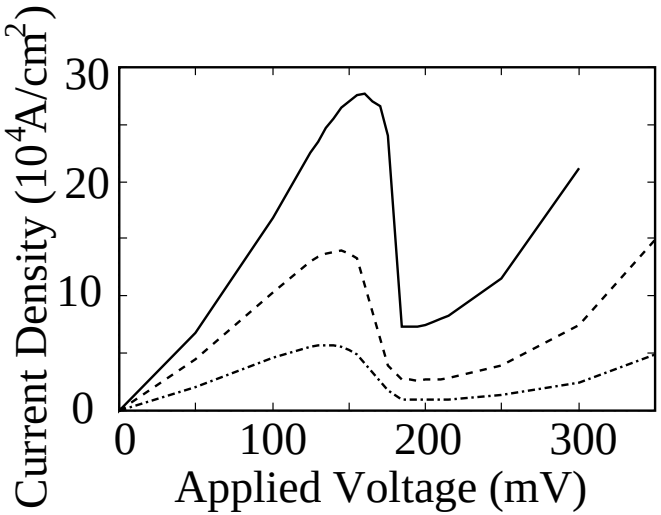

Fig. 2
Shi et al.
SSC

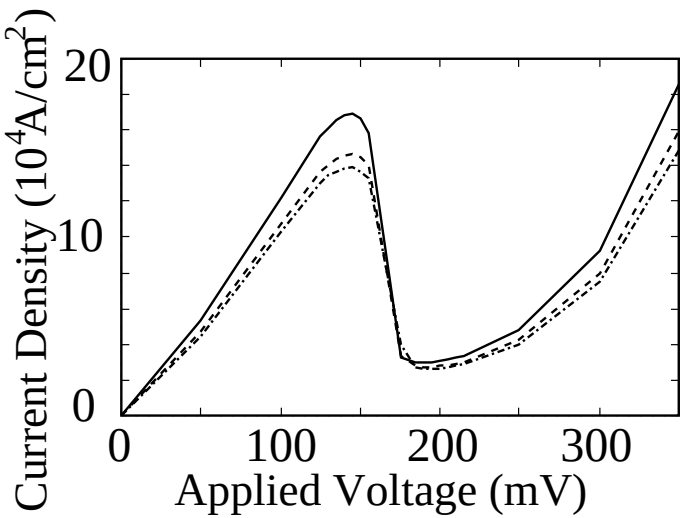

Fig. 3
Shi et al.
SSC